



Reliability of satellite precipitation observations in characterizing the spatiotemporal variations of rainfall erosivity over China

Qiao Liu, Fengrui Chen & Zengliang Guo

To cite this article: Qiao Liu, Fengrui Chen & Zengliang Guo (2025) Reliability of satellite precipitation observations in characterizing the spatiotemporal variations of rainfall erosivity over China, International Journal of Remote Sensing, 46:22, 8737-8761, DOI: [10.1080/01431161.2025.2572044](https://doi.org/10.1080/01431161.2025.2572044)

To link to this article: <https://doi.org/10.1080/01431161.2025.2572044>



Published online: 16 Oct 2025.



Submit your article to this journal [↗](#)



Article views: 38



View related articles [↗](#)



View Crossmark data [↗](#)



Reliability of satellite precipitation observations in characterizing the spatiotemporal variations of rainfall erosivity over China

Qiao Liu^{a,b}, Fengrui Chen^{a,b} and Zengliang Guo^{a,b}

^aState Key Laboratory of Spatial Datum, and Key Laboratory of Geospatial Technology for the Middle and Lower Yellow River Regions, Ministry of Education, Henan University, Zhengzhou, Henan, China; ^bCollege of Remote Sensing and Geoinformatics Engineering, Faculty of Geographical Science and Engineering, Henan University, Kaifeng, Henan, China

ABSTRACT

Rainfall erosivity (RE), a core indicator for soil erosion risk assessment, plays a crucial role in understanding soil erosion processes. While recent advances in satellite-based precipitation observations have enabled novel approaches for RE estimation across various scales, significant challenges remain. The inherent spatiotemporal variability of precipitation introduces considerable uncertainties in satellite-derived precipitation data, consequently making the reliability of satellite-derived rainfall erosivity estimates (SREE) in both temporal and spatial dimensions unclear and necessitates systematic evaluation. In this study, we comprehensively assessed the reliability of SREE in capturing RE spatiotemporal variations across the Chinese mainland at multiple temporal scales. The evaluation utilized seven widely used satellite precipitation products (SPPs) (TRMM-3B42, IMERG-Final, PERSIANN-CDR, GSMaP-Gauge, CHIRPS, CMORPH-BLD, and MSWEP), with RE derived from observations at over 2,400 meteorological stations as the benchmark. Key findings include: (1) significant differences exist in the reliability of RE estimates across different SPPs. RE estimates from IMERG-Final and CMORPH-BLD performed best, with median KGE and median SPAEF values greater than 0.5 in most basins, whereas those from PERSIANN-CDR performed worst, with median values below 0.5; (2) SREE perform significantly better in capturing the temporal variations of RE than its spatial variations, especially at monthly and seasonal scales, and they show great uncertainty in identifying spatial variations of RE in most basins; (3) SREE struggle to capture RE's temporal dynamics in the basins of western China but performs reliably in the basins of southeaster China, where most median KGE values exceed 0.5; and (4) SREE demonstrate higher uncertainty in winter, while showing relatively superior reliability in spring and autumn. The present study provides valuable references and operational guidance for expanding and deepening the applications of SREE in fields such as environmental science, agriculture, and soil and water conservation.

ARTICLE HISTORY

Received 4 June 2025
Accepted 4 October 2025

KEYWORDS

Rainfall erosivity; satellite-derived precipitation observations; reliability; temporal variation; spatial variation

1. Introduction

Soil erosion is one of the most severe threats to global food production and has become a critical constraint to sustainable development worldwide (Bezak et al. 2024; Borrelli et al. 2023; Hou et al. 2020). Rainfall-induced erosion is the predominant form of soil erosion and poses a significant threat to land productivity and ecological balance (Wang et al. 2024; Yu et al. 2019). Rainfall erosivity (RE), a key indicator for measuring the potential of rainfall to erode surface soil, provides an effective tool for assessing and predicting soil erosion risks (Nearing et al. 2017). Given the pronounced spatiotemporal heterogeneity of precipitation, accurate estimation of RE's spatial distribution is essential for soil conservation, agriculture planning, and ecological protection (Xu et al. 2019; Zhang et al. 2021). It also provides critical guidance for monitoring, forecasting, and management regional soil erosion.

The high spatiotemporal heterogeneity of precipitation directly leads to significant variations in RE across space and time. For example, in the karst region of Southwest China, the annual RE exhibits a distinct spatial pattern with higher values in the south and lower values in the north, while RE in summer is typically several times higher than that in winter (Xu et al. 2023). Notably, due to the skewed distribution characteristics of precipitation, although extreme precipitation events occur infrequently, their contribution to soil erosion is extremely significant (Yan et al. 2024). These factors pose substantial challenges to the accurate estimation of RE.

Compared with conventional ground-based precipitation observations, satellite precipitation observations offer significant advantages including global coverage, continuous monitoring, and high temporal resolution (Chen and Gao 2018; Pradhan et al. 2022; Song et al. 2024), providing new opportunities for regional and global RE estimation (Bezak, Borrelli, and Panagos 2022; Gebremicael et al. 2019; Tan et al. 2015). However, it should be emphasized that satellite precipitation products (SPPs) contain inherent spatiotemporal uncertainties. A large number of studies have been conducted worldwide to evaluate the uncertainties of SPPs in regions such as the Chinese mainland (Chi et al. 2023; Zhang et al. 2020) and the United States (Alnahit, Mishra, and Khan 2020). Generally, these uncertainties mainly stem from systematic errors in retrieval algorithms, physical limitations of sensor detection accuracy, and the inherent spatiotemporal variability of precipitation processes (Bartsotas et al. 2018; Chi et al. 2023; Taghizadeh et al. 2021; Yu et al. 2020). This is particularly evident in complex terrain areas, surface cover types, local topographic variations, and meteorological conditions can further amplify this uncertainty (Golian et al. 2015; Song et al. 2024; Zhan et al. 2023). Given that the primary purpose of developing satellite precipitation products is to meet application requirements across various fields, recent years have witnessed a growing body of research evaluating the uncertainties associated with these datasets in practical applications. Examples of these applications include drought monitoring (Zhang et al. 2022; Zhang, Wu, Yeh, Li, Hu, Feng, and Jun 2022), hydrological modelling (Chen et al. 2022; Zhang, Wu, Yeh, Li, Hu, Feng, and Lei 2022), and the assessment of extreme precipitation events (Yang et al. 2024; Y. Zhang et al. 2022). Unlike these studies, erosion is primarily driven by heavy rainfall, and a nonlinear and complex relationship exists between precipitation and erosive energy (Song et al. 2024). It is therefore necessary to systematically evaluate the reliability of satellite-derived RE estimates (SREE).

Several studies have initiated assessments of SREE uncertainty. Li, Li, and Lin (2020) and Teng et al. (2017) estimated RE using 3B42, preliminarily demonstrating the feasibility of deriving RE from satellite precipitation data. Chen et al. (2021) evaluated the performance of Tropical rainfall measuring mission Multi-satellite Precipitation Analysis 3B42 (TMPA 3B42) and Integrated Multi-satellitE Retrievals for GPM Final Run (IMERG-F) in estimating multi-year average rainfall erosivity. Bezak, Borrelli, and Panagos (2022) and Das et al. (2024) investigated the application of SPP in RE estimation worldwide. However, these assessments were predominantly conducted from a holistic perspective, without separately examining their performance across temporal and spatial dimensions or analysing the differences between them. In practical applications, however, data users are often more concerned with both spatial and temporal variation patterns of RE. To date, the reliability of SREE in characterizing these variations remains unclear. Given the spatiotemporal heterogeneity and skewed distribution characteristics of RE, it is necessary to separately and thoroughly investigate the uncertainty of SREE from both temporal and spatial dimensions. Furthermore, the multi-scale nature of RE necessitates uncertainty assessments across multiple temporal scales. Currently, such studies remain scarce, leaving the reliability of SREE in capturing RE's spatiotemporal variations insufficiently quantified. Additionally, with ongoing advancements in satellite precipitation retrieval techniques, new SPPs continue to emerge, each exhibiting unique advantages. This evolving landscape underscores the need to expand beyond evaluations of individual SPP. A systematic comparison of SREE derived from multiple SPPs would provide more robust insights into their reliability and applicability.

This study aims to assess the reliability of SREE in characterizing the spatiotemporal variations of RE. To achieve this, we evaluated the uncertainty of SREE derived from seven mainstream SPPs in representing the temporal and spatial variations of RE, using RE obtained from dense observations at over 2400 rain gauges as benchmarks. The analysis focuses on ten major river basins in the Chinese mainland from 2001 to 2018 and examines SREE performance across multiple temporal scales for a comprehensive assessment.

2. Study area and datasets

2.1. Study area

China, experiencing some of the world's most severe soil erosion, features complex and diverse topography, encompassing five primary terrain types: plains, mountains, hills, basins, and plateaus. The terrain generally follows an elevational gradient descending from west to east (Chen, Li, and Wang 2025; Wang, Shunlin, and Peijun 2022). Precipitation distribution shows distinct regional and seasonal variations, with relatively abundant annual rainfall in southeastern China compared to northwestern inland areas, and concentrated summer precipitation (Jiang et al. 2021; Xu et al. 2024). To comprehensively evaluate the applicability of SPPs for RE across the Chinese mainland, we divided the study area into ten river basins based on primary watershed boundaries: Yangtze (YTRB), Yellow (YRB), Huaihe (HRB), Haihe (HARB), Pearl (PRB), Songhua (SRB), Liaohe (LRB), Southeast (SERB), Southwest (SWRB), and Northwest (NWRB) river basins (Figure 1).

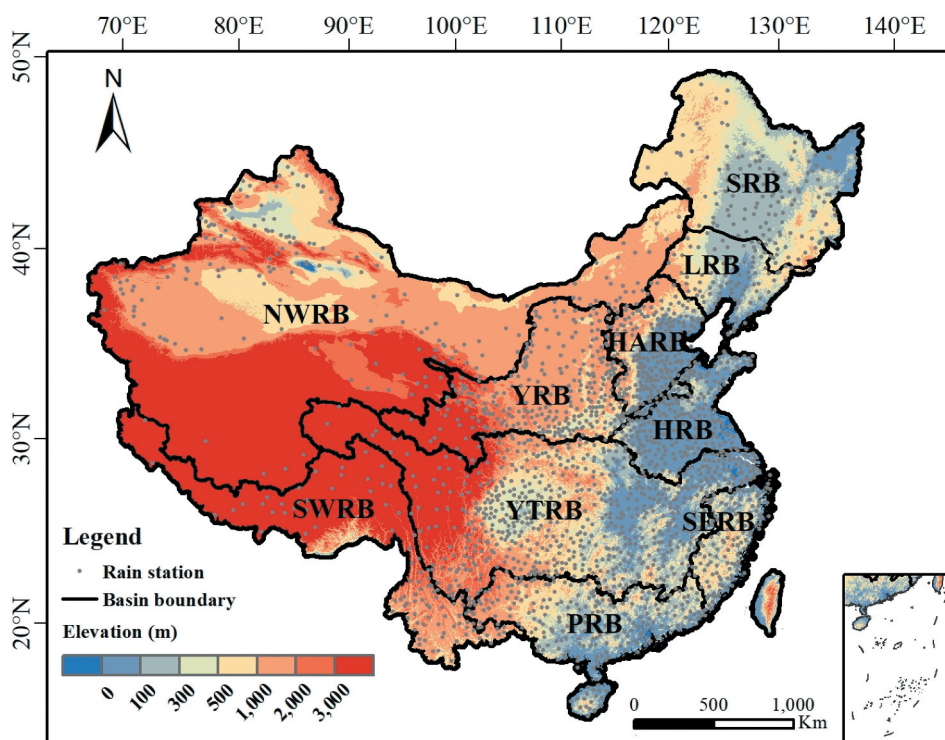


Figure 1. Spatial distribution of the ten major river basins and meteorological stations.

2.2. Datasets

Seven SPPs were selected to estimate RE, representing the state-of-the-art in global precipitation monitoring technologies. These SPPs include: TRMM-3B42, IMERG-Final, Precipitation Estimation from Remotely Sensed Information using Artificial Neural Networks – Climate Data Record (PERSIANN-CDR), Global satellite mapping of precipitation gauge-adjusted version (GSMaP-Gauge), Climate hazards group infrared precipitation with stations (CHIRPS), Climate prediction centre MORPHing technique bias-corrected product (CMORPH-BLD); and Multi-Source weighted-ensemble precipitation (MSWEP). TRMM-3B42 is a precipitation data product derived from the Tropical Rainfall Measuring Mission (TRMM) satellite. It integrates data from TRMM's Microwave Imager (TMI) and Precipitation Radar (PR) with other satellite observations and ground-based measurements through a series of algorithms to estimate precipitation. IMERG-Final is the final product of the Integrated Multi-satellite Retrievals for GPM (IMERG), which merges observations from the GPM core satellite and multiple other satellites. Ground-based gauge data are incorporated for calibration. The process involves various algorithms, including cloud motion vector propagation, to enhance the accuracy of precipitation estimates. PERSIANN-CDR is a satellite-based precipitation product. It primarily utilizes GridSat-B1 infrared data derived from ISCCP B1 and GPCP version 2.2 merged data, combined with artificial neural network algorithms for precipitation estimation. GSMaP-Gauge is part of the Global Satellite

Mapping of Precipitation (GSMaP) project. It integrates satellite observations with ground-based gauge data. The product employs satellite precipitation estimation algorithms and gauge data fusion to generate high-resolution precipitation data. CHIRPS is generated by combining satellite infrared data, gauge observations, and other meteorological data. It uses an improved precipitation estimation algorithm to integrate and calibrate different data sources. CMORPH-BLD is generated using a morphing technique that integrates satellite precipitation estimates and gauge data. The product employs morphological methods for spatiotemporal interpolation and calibration of precipitation data. MSWEP integrates multiple precipitation data sources, including satellite observations, gauge measurements, and meteorological model data. A weighted ensemble method is used to generate the final product, with quality assessments and weight assignments for each data source. These SPPs were selected based on their data availability covering our study period (2001–2018) and their widespread application in climatic and hydrological research. [Table 1](#) summarizes the key characteristics of these SPPs, including sensor Type, spatial-temporal resolutions, and coverage domains.

Daily precipitation records covering the period 2001–2018 were obtained from the China Meteorological Data Sharing Network (<https://data.cma.cn/>). The dataset encompasses observations from a comprehensive network of over 2400 meteorological stations distributed across the Chinese mainland. Since these data had undergone rigorous quality control prior to release (R. Yu et al. 2007), no additional processing was performed. As shown in [Figure 1](#), the meteorological stations exhibit a distinct spatial distribution pattern, with higher density in eastern China than in western regions.

3. Method

3.1. Data preprocessing

To guarantee the robustness of our analyses, we implemented the following data processing protocol. First, to minimize potential errors arising from data gaps, we first excluded meteorological stations with missing observations exceeding 5% of the study period, yielding a final dataset of over 2,200 stations. Next, for alignment purposes, the spatial resolution of IMERG-Final and MSWEP was resampled to 0.25° (Keikhosravi-Kiany et al. 2021), matching the other five SPPs. Finally, average precipitation values were computed by aggregating observations from multiple meteorological stations within each 0.25° × 0.25° grid cell (Duan et al. 2016; Kiany et al. 2020).

Table 1. Summary of the seven types of SPPs used in this study.

SPPs	Sensor type	Temporal resolution	Spatial resolution	Coverage	Reference
TRMM-3B42	Combined	3-hourly	0.25°	50°N-S	Huffman et al. (2007)
IMERG-Final	Combined	Half-hourly	0.1°	60°N-S	Huffman et al. (2020)
PERSIANN-CDR	IR	Daily	0.25°	60°N-S	Ashouri et al. (2015)
GSMaP-Gauge	Combined	Hourly	0.25°	60°N-S	Tashima et al. (2020)
CHIRPS	IR	Daily	0.25°	50°N-S	Funk et al. (2015)
CMORPH-BLD	Combined	Half-hourly	0.25°	60°N-S	Joyce et al.(2004)
MSWEP	Combined	3-hourly	0.1°	60°N-S	Beck et al. (2019)

3.2. Rainfall erosivity model

A daily rainfall erosivity model developed by Xie et al. (2016) was utilized to estimate RE from both gauge precipitation observation and SPPs. This model has been widely adopted due to its demonstrated high accuracy and effectiveness in China, as follows:

$$R_i = \alpha \sum_{j=1}^k P_d 1.7265 \quad (1)$$

Where R_i represents the rainfall erosivity of the i -th half month in a year (units: MJ mm (hm² h)⁻¹); k is the number of days with erosive rainfall in half a month, P_d represents the daily rainfall amount on the j -th day with erosive rainfall, where erosive rainfall is defined as ≥ 10 mm (day)⁻¹; α is a dimensionless parameter: $\alpha = 0.3937$ for the warm season (May – September) and $\alpha = 0.3101$ for the cold season (October – April). Monthly RE was calculated by summing the half-monthly values. Seasonal and annual RE were obtained by aggregating monthly values within the respective time periods. Based on this model, SREE and RE_o are computed independently, using seven SPPs and station precipitation observations, respectively.

3.3. Quantitative evaluation

This study focuses on the reliability of SREE in characterizing the spatial and temporal variations of RE. Specially, we evaluated seven SREE against RE_o across 10 major basins in China at monthly, seasonal, and annual scales to ensure comprehensive exploration. Two integrated metrics – the Kling-Gupta efficiency (KGE) (Gupta et al. 2009) and SPAtial Efficiency metric (SPAEF) (Koch, Cüneyd Demirel, and Stisen 2018) – were used to quantify SREE's performance in capturing temporal and spatial variations of RE, respectively. The KGE consists of three components measuring temporal consistency, bias, and variability between the estimates and reference values:

$$KGE = 1 - \sqrt{(C - 1)^2 + (B - 1)^2 + (R - 1)^2} \quad (2)$$

$$C = \rho(s_t, o_t), \quad B = \frac{\mu_{s_t}}{\mu_{o_t}} \text{ and } R = \frac{\sigma_{s_t}/\mu_{s_t}}{\sigma_{o_t}/\mu_{o_t}} \quad (3)$$

Where s_t and o_t represent the temporal series of SREE and RE_o, respectively; μ and σ denote their mean and standard deviation, respectively; and C , B , and R are Pearson correlation coefficient, bias ratio, and ratio of coefficient of variation. Similar to KGE, SPAEF also comprises three components:

$$SPAEF = 1 - \sqrt{(C' - 1)^2 + (R' - 1)^2 + (B' - 1)^2} \quad (4)$$

$$C' = \rho(s_s, o_s), \quad B' = \frac{\sum_{j=1}^n \min(K_j, L_j)}{\sum_{j=1}^n K_j}, \text{ and } R' = \frac{\sigma_{s_s}/\mu_{s_s}}{\sigma_{o_s}/\mu_{o_s}} \quad (5)$$

Where s_s and o_s represent the spatial patterns of SREE and RE_o, respectively; C' , B' , and R' are their Pearson correlation coefficient, percentage of histogram intersection, and ratio of the coefficient of variation. The closer both KGE and SPAEF values are to 1, the better the model performance.

4. Results

4.1. Spatial distribution of SREE

Figures 2 and 3 display the multi-year averaged SREE derived from seven SPPs for January and August, respectively. Generally, the spatial distribution of RE shows considerable variability, with values increasing from the northwest to the southeast. In January, RE values are low across most basins, indicating weaker erosivity during winter. RE values in most of NWRB are below $100 \text{ MJ}\cdot\text{mm} (\text{hm}^2 \cdot \text{h}\cdot\text{yr})^{-1}$, while those in PRB, SERB, and the southeastern part of YTRB exceed $200 \text{ MJ}\cdot\text{mm} (\text{hm}^2 \cdot \text{h}\cdot\text{yr})^{-1}$. In contrast, August shows substantially higher SREE across most basins due to greater rainfall. Although NWRB largely maintains RE below $100 \text{ MJ}\cdot\text{mm} (\text{hm}^2 \cdot \text{h}\cdot\text{yr})^{-1}$, eastern China experiences values surpassing $800 \text{ MJ}\cdot\text{mm} (\text{hm}^2 \cdot \text{h}\cdot\text{yr})^{-1}$. It should be noted that spatial patterns of SREE vary significantly among SPPs. In January, MSWEP and PERSIANN-CDR yield considerably lower RE in southeastern China compared to other products. By August, however, TRMM-3B42, CHIRPS, and IMERG-Final exhibit substantially higher RE ($> 1000 \text{ MJ}\cdot\text{mm} (\text{hm}^2 \cdot \text{h}\cdot\text{yr})^{-1}$) throughout southern China compared to the remaining SPPs.

4.2. Performance of monthly SREE

Figure 4 demonstrates the capability of SREE derived from seven SPPs to characterize the temporal variations of monthly RE across ten river basins in the Chinese mainland. Overall,

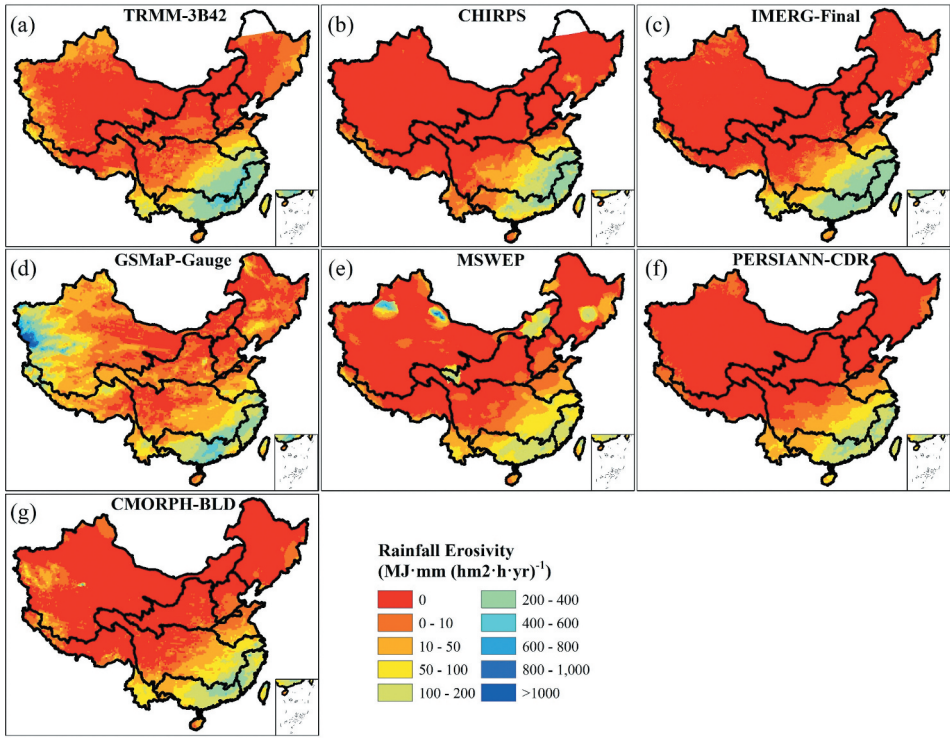


Figure 2. Spatial distribution of the multi-year averaged SREE in January.

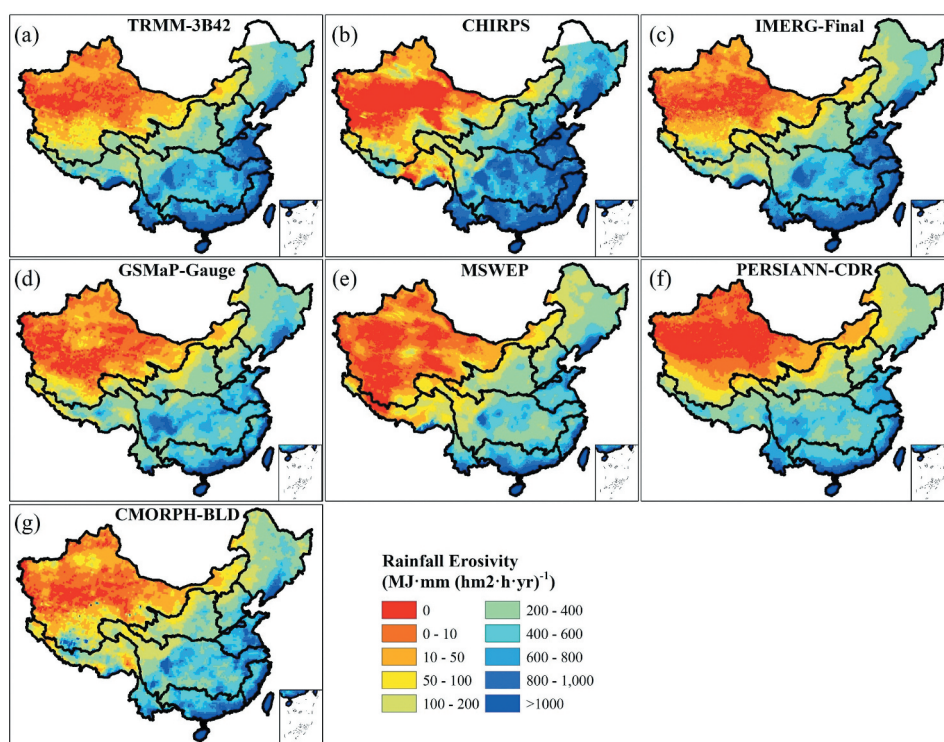


Figure 3. Spatial distribution of the multi-year averaged SREE in August.

SREE from most SPPs effectively capture the temporal variations of monthly RE, with median KGE values exceeding 0.5 in most basins. Among these products, IMERG-Final and CMORPH-BLD demonstrate the best performance, with median KGE values ranging from 0.7 to 0.8 across most study areas. The next best performers are TRMM-3B42, MSWEP, CHIRPS, and GSMap-Gauge, while PERSIANN-CDR exhibits the lowest reliability with median KGE values predominantly below 0.5. The reliability of SREE shows significant spatial heterogeneity in characterizing the temporal variations of monthly RE. Particularly poor performance is observed in the basins of northern China, especially in NWRB where median KGE values remain consistently below 0.4. This limitation is primarily attributed to the exceptionally low consistency (C) between SREE and RE within this basin. In contrast, SREE more accurately characterize the temporal changes in monthly RE in the south-eastern coastal areas of China, where most estimates achieve median KGE values above 0.5. Notably, the relative performance ranking of SREE varies regionally. For example, TRMM-3B42 outperforms IMERG-Final in HARB, while performing worse in other basins.

Figure 5 evaluates the ability of seven SREE to capture monthly RE spatial variations across China. Compared to their performance in characterizing temporal variations (Figure 4), seven SREE generally demonstrate reduced accuracy and have great uncertainty in representing spatial variations. This mainly stems from the fact that the spatial consistency (C') between SREE and RE is significantly lower than their temporal consistency (C) (Figure 4). Overall, CMORPH-BLD shows the highest performance, with median SPAEF values above 0.5 in most basins. The subsequent ranking includes MSWEP, IMERG-

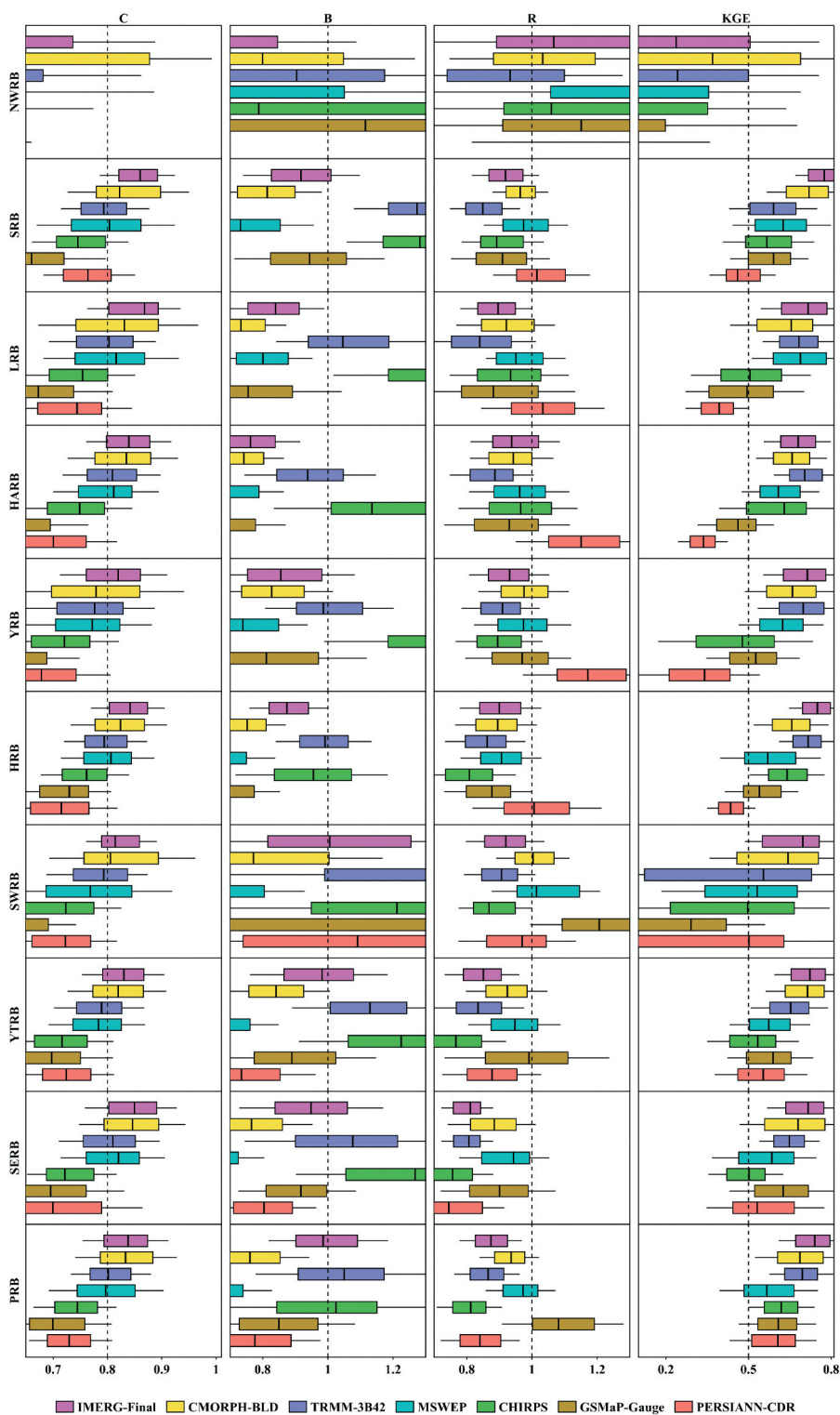


Figure 4. Performance of seven SREE to characterize the temporal variations of monthly RE on an annual cycle.

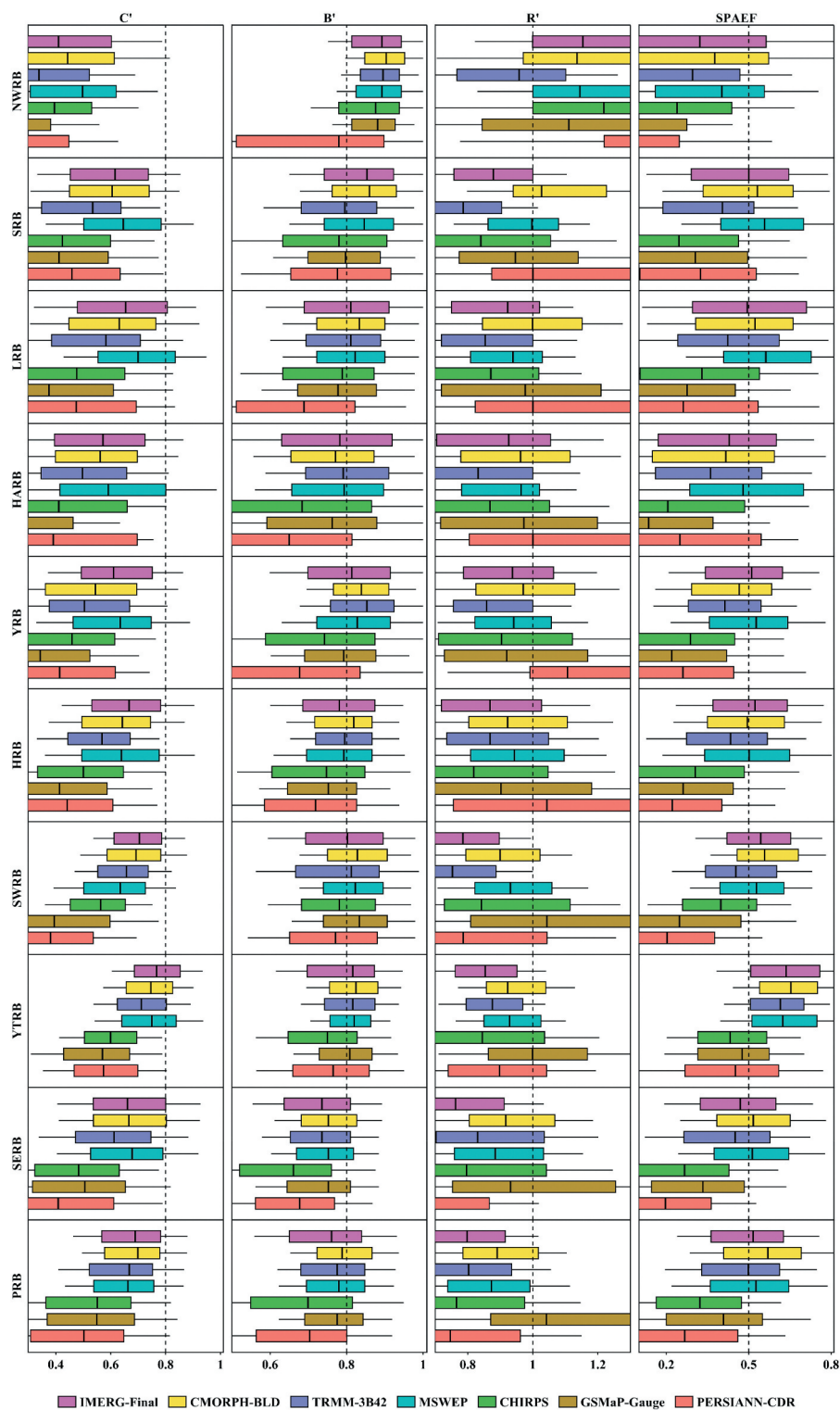


Figure 5. Performance of seven SREE to characterize the spatial variation of monthly RE on an annual cycle.

Final, TRMM-3B42, CHIRPS, and GSMap-Gauge. PERSIANN-CDR performs most poorly, with median SPAEF values consistently below 0.3. Spatially, SREE relatively reliably identifies monthly RE spatial variations in YTRB and the PRB compared to other basins. It should be noted that MSWEP achieves higher median SPAEF values than CMORPH-BLD in YRB, HARB, LRB, SRB, and NWRB, indicating basin-dependent performance variation among SREE.

Figure 6 illustrates seasonal variations in the performance of seven SREE for characterizing monthly RE temporal changes. The SREE demonstrate peak performance in autumn, with median KGE values exceeding 0.5 for most estimates, while winter shows the weakest performance with median KGE values generally below 0.5. IMERG-Final maintains superior performance across all seasons, achieving median KGE values above 0.5 in most basins. In contrast, PERSIANN-CDR remains the lowest-performing product, typically showing negative median KGE values. NWRB exhibits particularly poor performance across seasons, rarely exceeding 0.3 in median KGE values. Notably, the characterization ability of SREE also varies across different seasons. For example, in LRB and SRB, MSWEP performs better in spring than in autumn.

The capability of seven SREE to represent monthly RE spatial variations exhibits marked seasonal variability, as illustrated in Figure 7. Distinct from their temporal variation performance (Figure 6), these SREE demonstrate optimal performance during spring, with median SPAEF values fluctuating around 0.5. Winter exhibits notably poorer performance compared to Spring, with most estimates showing median SPAEF values below 0.5. CMORPH-BLD generally emerges as the top-performing product, consistently maintaining median SPAEF values above 0.5, while PERSIANN-CDR demonstrates the weakest performance with almost median SPAEF values almost always below 0.5. Additionally, the capability of SREE to characterize monthly RE spatial variations varies seasonally. For instance, CHIRPS outperforms GSMap-Gauge in most river basins during spring, whereas GSMap-Gauge shows better performance in summer.

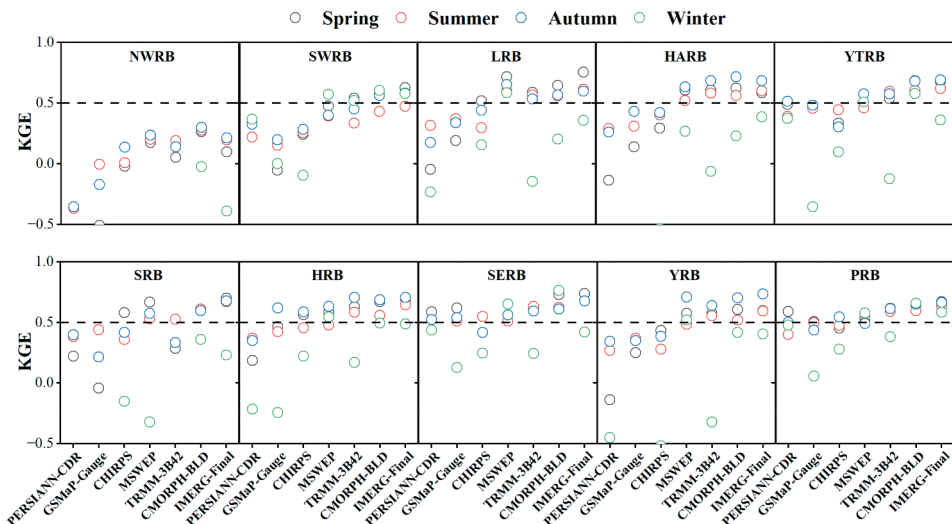


Figure 6. Performance of seven SREE to characterize the temporal variation of monthly RE on a seasonal cycle.

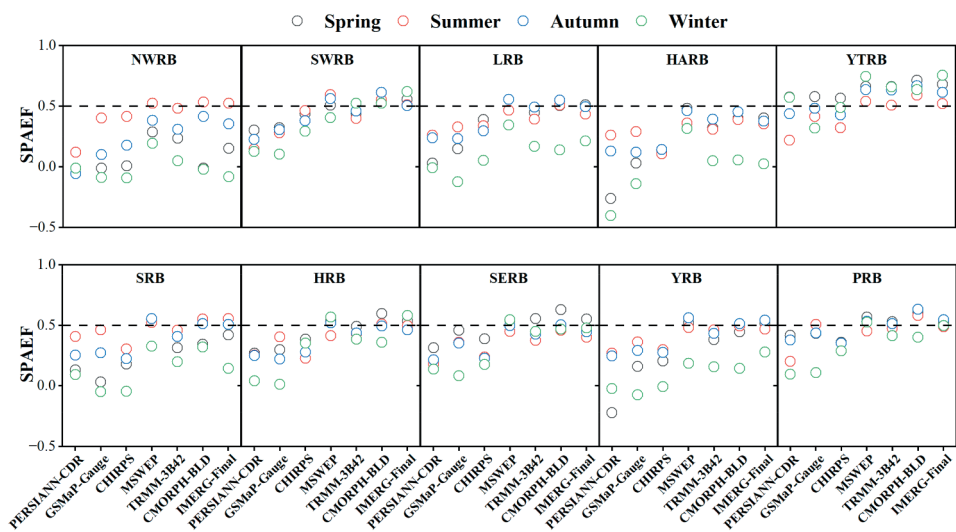


Figure 7. Performance of seven SREE to characterize the spatial variation of monthly RE on a seasonal cycle.

4.3. Performance of seasonal SREE

Figure 8 evaluates the capacity of seven SREE to identify seasonal RE temporal variations across an annual cycle. Compared to their performance in capturing monthly variation (Figure 4), SREE demonstrate significantly enhanced accuracy for seasonal RE characterization, with median KGE values above 0.6 for most SPPs. IMERG-Final emerges as the top performer, attaining median KGE values above 0.7 across multiple basins and exceeding 0.8 in certain regions. CMORPH-BLD and TRMM-3B42 follow closely, showing consistently higher accuracy than other products. Intermediate performance is observed for MSWEP, CHIRPS, and GSMaP-Gauge (median KGE: 0.5–0.7), while PERSIANN-CDR trails significantly with median KGE values around 0.5. The poorest performance occurs in NWRB (median KGE values < 0.5), with similarly suboptimal results in SWRB. Conversely, more stable performance appears across the remaining basins. Notably, TRMM-3B42 surpasses IMERG-Final in LRB, HARB, and YRB, revealing basin-dependent performance variations among SPPs.

The reliability of SREE in characterizing seasonal RE spatial variation is evaluated in Figure 9. Compared to the monthly RE analysis (Figure 5), SREE demonstrate significantly improved spatial characterization ability, mainly attributed to their improved spatial consistency (C'). CMORPH-BLD, IMERG-Final, and MSWEP stand out with the highest capacity, achieving median SPAEF values above 0.5 in most basins, followed by TRMM-3B42. In contrast, PERSIANN-CDR, CHIRPS, and GSMaP-Gauge exhibit relatively weaker performance. Spatially, NWRB continues to show the lowest accuracy, with all seven SREE exhibiting median SPAEF values below 0.5. Reliable characterization occurs in the YTRB, PRB, HARB, YRB, and LRB, where CMORPH-BLD demonstrates superior performance. These results reveal distinct basin-dependent variations in the spatial characterization capability of seasonal SREE.

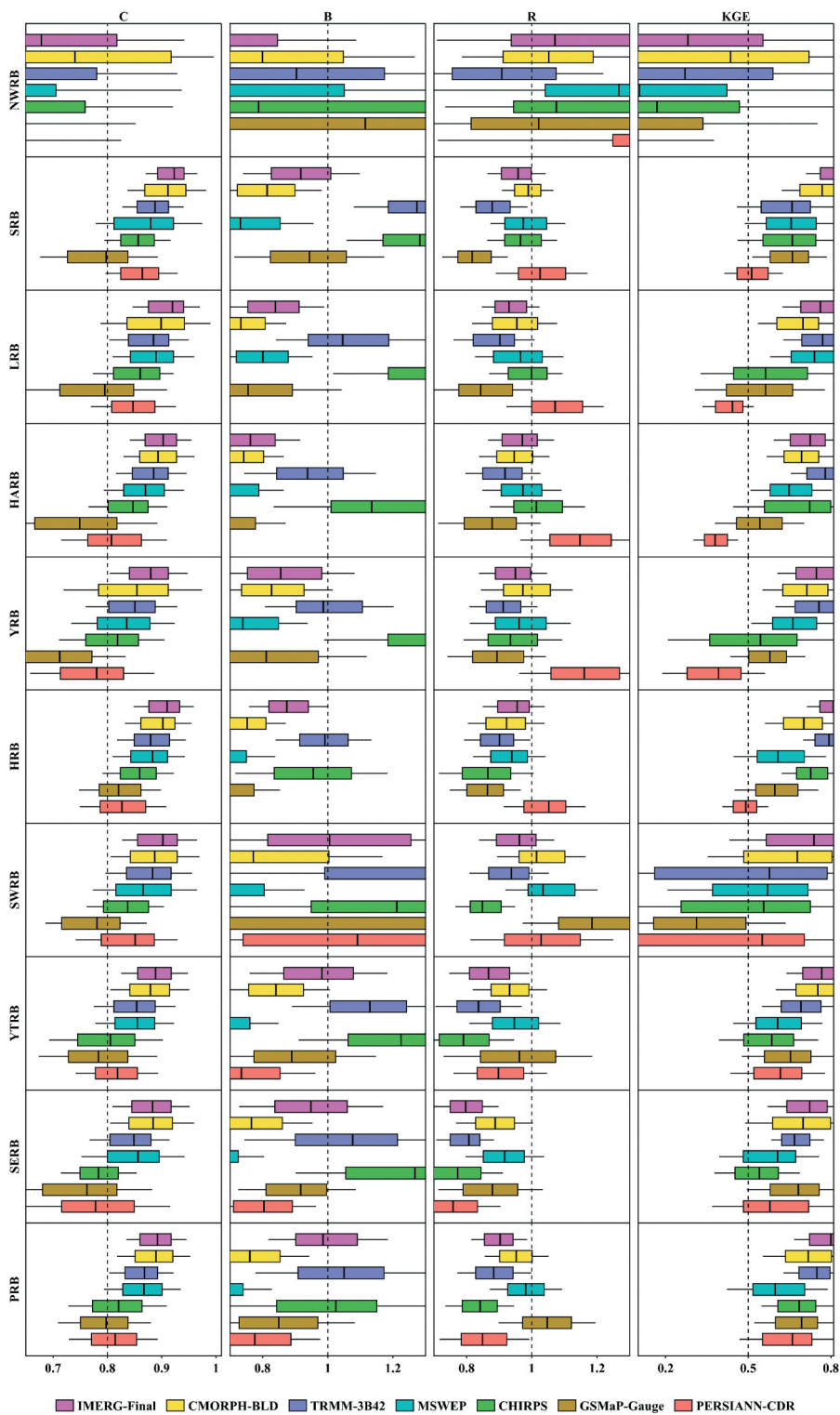


Figure 8. Performance of seven SREE to characterize the temporal variation of seasonal RE on an annual cycle.

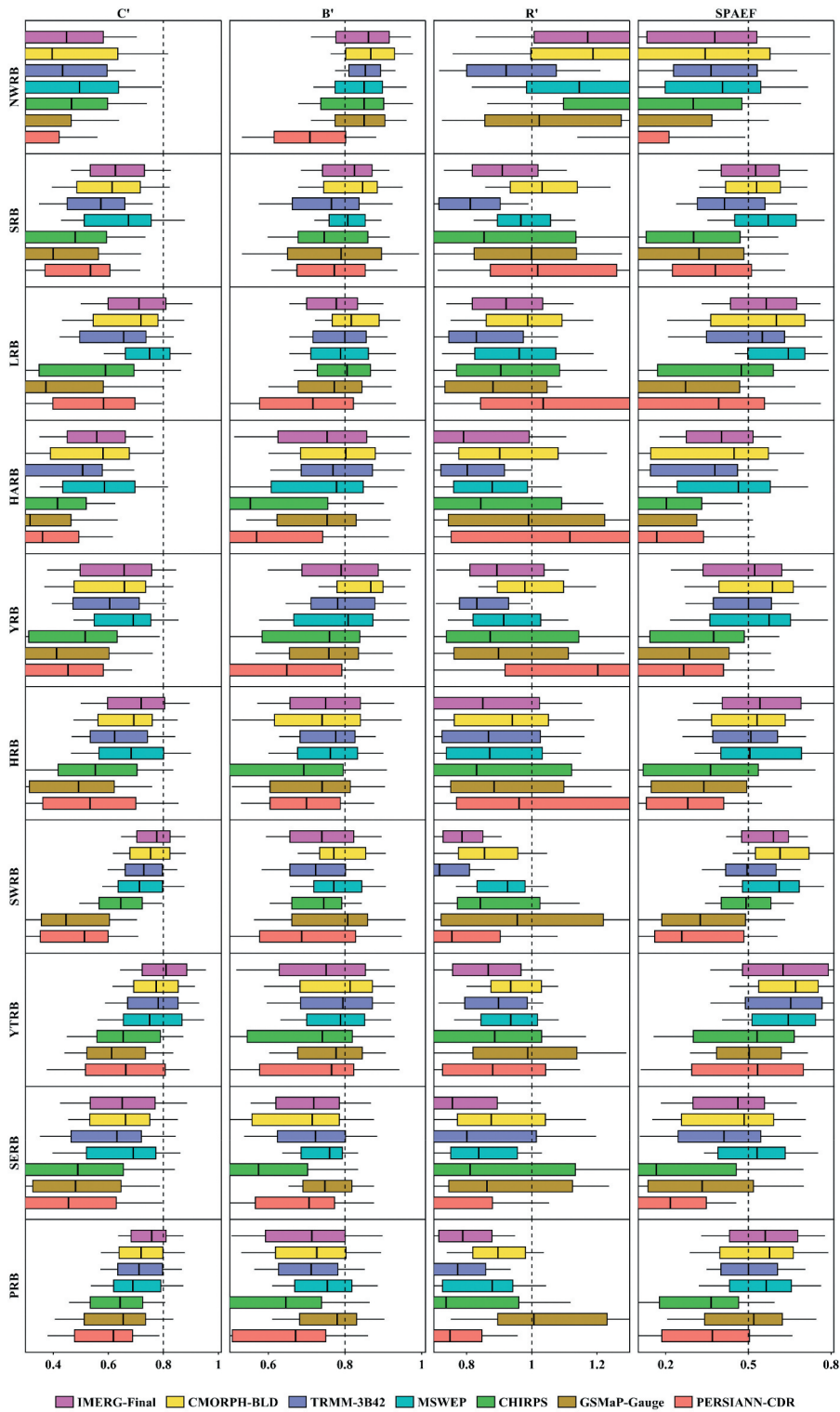


Figure 9. Performance of seven SREE to characterize the spatial variation of seasonal RE on an annual cycle.

Figure 10 evaluates the reliability of SREE in characterizing seasonal RE temporal variations. The method shows reduced effectiveness for seasonal characterization compared to monthly RE analysis (Figure 6), with accuracy peaking in autumn and reaching its lowest level in winter. Overall, IMERG-Final achieves the strongest performance, with median KGE values predominantly exceeding 0.5, while PERSIANN-CDR performs the weakest, with median KGE values largely below 0.4. Spatially, SPPs show superior performance in the southeast region compared to the northwest. Seasonal variations in performance are also evident; for example, CMORPH-BLD performs best in HARB during autumn, whereas IMERG-Final excels in summer.

Figure 11 demonstrates significant seasonal variations in SREE's ability to characterize the spatial patterns of seasonal RE. Compared to the monthly RE characterization analysis (Figure 7), the spatial characterization ability of seasonal RE shows an overall improving trend, enabling more reliable RE depiction. However, performance declines in certain basins (YTRB, SRB, and SERB) during autumn. SREE performance peaks in spring and reaches its lowest level in winter. CMORPH-BLD performs best with SPAEF medians predominantly above 0.5, while PERSIANN-CDR shows the weakest performance with most SPAEF medians below 0.4. Notably, SREE performance exhibits high spatial variability, with generally poor results in NWRB. The strongest performance occurs in YTRB during spring, where all seven SREE yield SPAEF medians above 0.5.

4.4. Performance of annual SREE

The ability of seven SREE to characterize annual RE temporal variation shows notable decline when compared to their performance for monthly and seasonal RE (Figures 4 and 8), as shown in Figure 12. Fewer SREE attain median KGE values above 0.5. IMERG-Final, CMORPH-BLD, and TRMM-3B42 maintains superior performance, with most median KGE

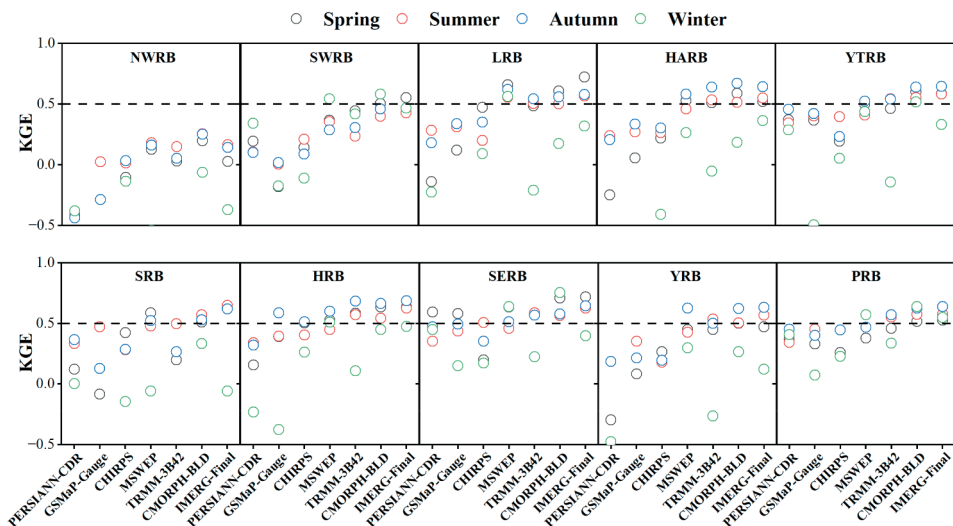


Figure 10. Performance of seven SREE to characterize the temporal variation of seasonal RE on a seasonal cycle.

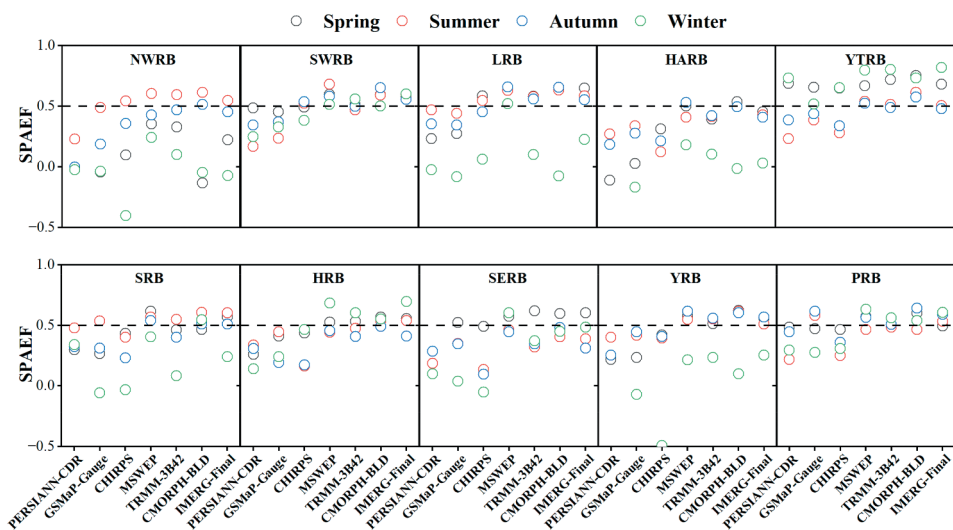


Figure 11. Performance of seven SREE to characterize the spatial variation of seasonal RE on a seasonal cycle.

values exceeding 0.5, while PERSIANN-CDR consistently underperforms, with all median KGE values below 0.4. Spatially, SWRB exhibits the best performance, where five SREE (IMERG-Final, CMORPH-BLD, TRMM-3B42, MSWEP, and GSMap-Gauge) showing median KGE values greater than 0.5. In contrast, NWEB displays the poorest performance, with all SREE falling below 0.4.

Figure 13 evaluates seven SREE performance in capturing spatial variations of annual RE. Unlike the temporal variation analysis (Figures 4, 8, and 12), their spatial characterization capability is generally superior to that for monthly and seasonal RE. Most SREE achieve median SPAEF values exceeding 0.5, with CMORPH-BLD emerging as the top performer across basins. PERSIANN-CDR and CHIRPS rank lowest, typically falling below 0.4. Significant regional variations exist among basins. Both SERB and HARB underperform, while SWRB shows relatively better results. Basin-specific performance variations are particularly notable, as different SREE achieve optimal performance in distinct basins. These findings demonstrate substantial basin-dependent variability in SREE annual spatial characterization effectiveness.

5. Discussion

The reliability of the seven mainstream SPPs assessed in this study varies significantly in characterizing the spatiotemporal variations of RE. Among them, IMERG-Final and CMORPH-BLD perform the best overall, while PERSIANN-CDR performs the worst. These performance differences mainly stem from the different data sources and retrieval algorithms used by each product. In addition to the bias correction performed with the Global Precipitation Climatology Centre precipitation dataset, IMERG-Final and CMORPH-BLD employ a multi-satellite joint retrieval technique that integrates microwave and infrared sensor data for precipitation estimation, achieving high temporal resolution (half-hourly)

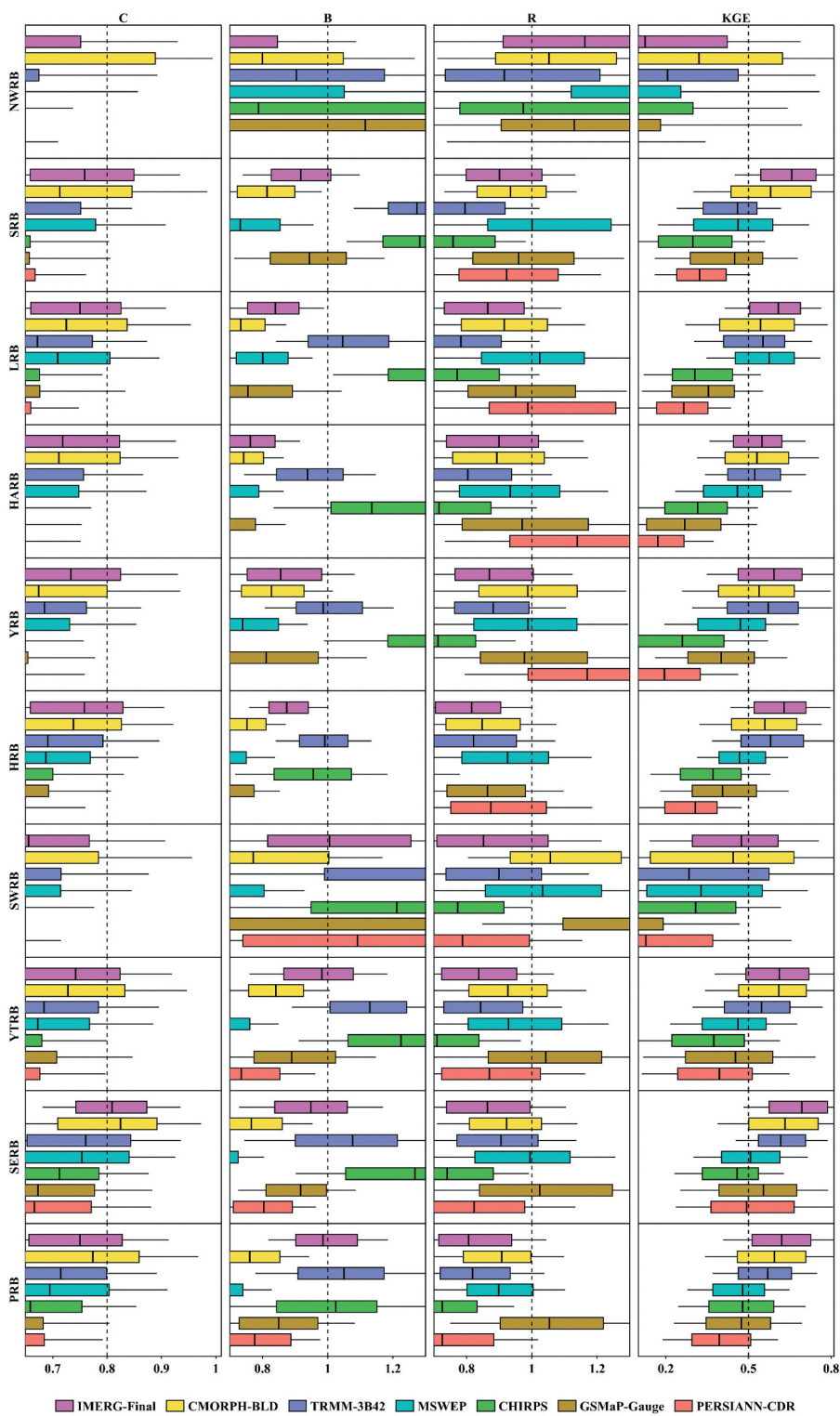


Figure 12. Performance of seven SRE to characterize the temporal variation of annual RE.

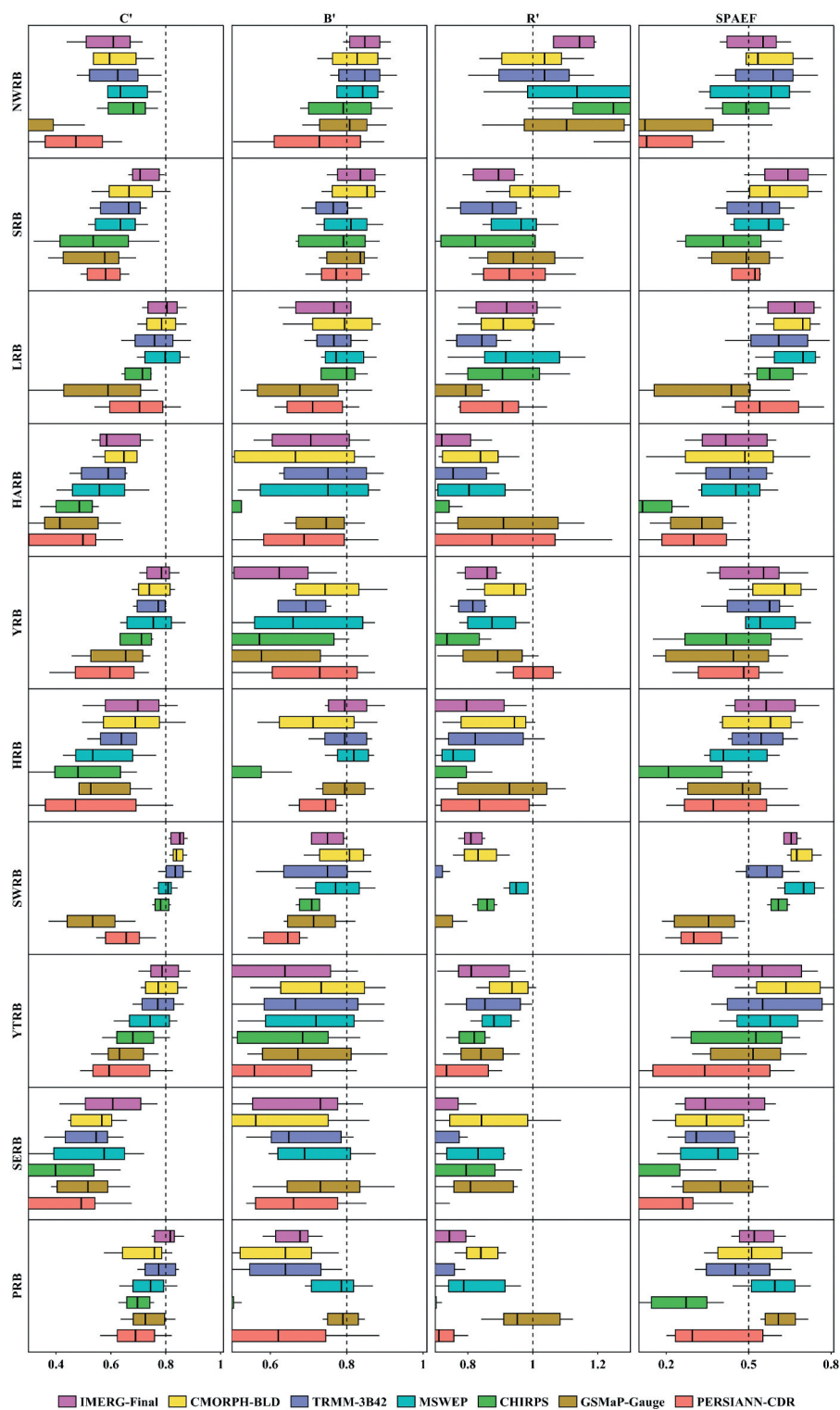


Figure 13. Performance of seven SREE to characterize the spatial variation of annual RE.

observations (Huffman et al. 2015; Joyce et al. 2004). IMERG-Final utilizes advanced precipitation-measuring radar that enables more accurate measurement of precipitation (Pradhan et al. 2022). CMORPH-BLD incorporates the Climate Prediction Center gauge-based daily precipitation for correction (Xie et al. 2017); compared to the monthly-scale correction methods commonly used by other precipitation products, this approach better preserves the diurnal variation characteristics of precipitation (Chi et al. 2023). These factors allow IMERG-Final and CMORPH-BLD to generate relatively accurate RE estimates. In contrast, PERSIANN-CDR relies solely on infrared sensor data, which is prone to causing great uncertainty due to the adoption of the indirect retrieval method (Miao et al. 2015). Additionally, its use of the Global Precipitation Climatology Project monthly 2.5° precipitation data for correction results in insufficient accuracy in daily precipitation estimation (Nguyen et al. 2018; Ruan et al. 2025), thereby affecting the accuracy of RE estimates. It is noteworthy that the performance ranking of SREE varies across regions. For example, the SREE generated by GSMaP-Gauge demonstrate better capability in capturing temporal variations of RE in the basins of southern China than those generated by CHIRPS, but perform relatively poorly in the basins of northern China. This finding is consistent with previous studies on SPP performance (Chen and Li 2016; Lei, Zhao, and Ao 2022), further confirming that different precipitation products have distinct regional advantages. Such regional reliability differences suggest that the most suitable SREE should be selected according to regional characteristics in practical applications.

Research findings demonstrate that SREE perform significantly better in characterizing the temporal variations of RE (particularly at monthly and seasonal scales) than in representing its spatial variations. This discrepancy occurs because the temporal consistency between SREE and RE is markedly higher than their spatial consistency (Figures 4 and 5). Since the temporal distribution of RE exhibits periodic characteristics (e.g. higher RE values in summer and lower values in winter), satellites can effectively capture both the temporal variation of precipitation and the consequent seasonal fluctuations of RE through high-frequency observations (Chen et al. 2022). However, in the spatial dimension, China's complex topography (e.g. karst landscapes in southwestern China and plateaus in the northwest) causes local precipitation to be influenced by micro-scale processes such as terrain uplift and surface cover (Chen, Wang, and Li 2024; Gan et al. 2020; Lu et al. 2018). A similar situation was also observed in the studies of Zhang et al. (2023) and Zhang et al. (2020), which found that for drought detection, SPPs face increased uncertainty in NWRB. This is because these areas have scarce precipitation and complex terrain. Meanwhile, the coarse spatial resolution of SPPs limits the accurate characterization of precipitation's spatial details. Together, these factors result in SREE's superior capability in characterizing temporal variations of RE compared to its spatial variations. Even in the best-performing SREE generated by IMERG-Final and CMORPH-BLD, substantial uncertainties persist across most river basins. This undoubtedly poses challenges when analysing SREE's spatial variation, necessitating extra caution in evaluating data reliability and stability to ensure the accuracy and credibility of the results. Furthermore, it is important to note that SREE's performance ranking differs between temporal and spatial dimensions. While IMERG-Final outperforms CMORPH-BLD in capturing temporal variations of RE, it is slightly inferior in resolving spatial variations.

In addition, the reliability of SREE exhibits significant spatiotemporal variations across regions and seasons. Specifically, seasonal variations show the poorest SREE performance

in winter, while spring and autumn demonstrate relatively better accuracy (Figures 6 and 7). This discrepancy is closely related to precipitation types and inherent limitations of satellite sensors. In northern China, winter precipitation occurs predominantly as snow, yet sensors in most SPPs show limited accuracy in solid precipitation retrieval (Lei, Zhao, and Ao 2022), resulting in higher uncertainties for RE estimation. Conversely, although high-frequency observations effectively capture summer convective precipitation, the spatial heterogeneity of extreme rainfall events (e.g. localized storms in southeastern China) remains challenging for satellite-based spatial representation. Spatially, SREE reliability is significantly higher in southeastern coastal areas (e.g. PRB) than in north-western China due to three key factors: (1) the substantial influence of complex topography on precipitation observation accuracy in NWRB (Lin et al. 2022; Zhan et al. 2023); (2) dense rain gauge networks combined with abundant precipitation in the basins of southeastern China, providing robust calibration references; and (3) persistent systematic biases in SPP algorithms for arid regions (Lu et al. 2018; Zhang et al. 2022). These factors collectively increase RE estimation uncertainties. The above spatiotemporal uncertainty patterns demonstrate that practical applications of SREE must account for both seasonal variations and topographic influences to ensure the reliability of SREE-based analyses.

Our study delineates the applicability domains of SREE across China, offering critical guidance for future research. For applications in southeastern China, SREE derived from IMERG-Final and CMORPH-BLD are recommended for RE temporal variation analysis. This finding is consistent with previous studies (Wan et al. 2025; Zhang, Wu, Yeh, Li, Hu, Feng, and Jun 2022; Zhang, Wu, Yeh, Li, Hu, Feng, and Lei 2022), which found both products performed well in the humid regions of southeast China, demonstrating high reliability in hydrological simulation and extreme precipitation monitoring. Future studies should prioritize machine learning-based multi-source data fusion approaches and season-specific algorithm optimization to enhance SREE's applicability in complex environments.

6. Conclusion

Although satellite precipitation observation provides unprecedented opportunities to estimate RE across regional and global scales, the reliability of SREE in capturing RE's spatiotemporal variations remains unclear due to the considerable uncertainties associated with SPPs. To address this gap, the present study conducts a comprehensive investigation into uncertainties in SREE derived from seven widely used SPPs for characterizing the temporal and spatial variations of RE across the Chinese mainland at multiple time scales, using the RE data from dense grounded observations as the benchmark. The main findings are summarized as follows:

- (1) Significant variations exist in the reliability of RE estimates across different SPPs. Among the seven evaluated SPPs, IMERG-Final and CMORPH-BLD exhibit the best performance, while PERSIANN-CDR shows the lowest reliability.
- (2) SREE perform significantly better at capturing the temporal variations of RE than its spatial variations. While SREE reliably identifies RE's temporal dynamics in most watersheds, its spatial representation remains reliable only in a few basins.

- (3) SREE exhibit significant differences in their ability to characterize RE across various temporal scales, with markedly better performance for monthly and seasonal PE estimates relative to annual-scale patterns.
- (4) The ability of SREE to characterize the temporal variation of RE exhibits significant spatial heterogeneity. In particular, SREE struggle to reliably capture RE's temporal dynamics in the basins of western China, especially in NWRB. In contrast, SREE demonstrate reliable performance in the basins of southeastern China, including YRB, PRB, and SERB.
- (5) SREE exhibit significant seasonal performance variations. They tend to demonstrate higher uncertainty in winter, while showing relatively superior reliability in spring and autumn.

This study, through comprehensive analysis, reveals the performance differences of various SPPs in estimating RE under different conditions, providing valuable references and operational guidance for expanding and deepening SREE applications. Reliable PE estimation requires comprehensive consideration of three key factors: SPPs accuracy characteristics, regional geoclimatic features, and appropriate temporal-scale selection. This ensures the reliability of the analysis results.

Disclosure statement

No potential conflict of interest was reported by the author(s).

Funding

This research was funded by the National Natural Science Foundation of China [grant number 42571447], the Dabieshan National Observation and Research Field Station of Forest Ecosystem at Henan, the Natural Science Foundation of Henan Province [222300420419], and the High Resolution Satellite Project of the State Administration of Science, Technology and Industry for National Defense of PRC [80Y50G19-9001-22/23].

References

- Alnahit, A. O., A. K. Mishra, and A. A. Khan. 2020. "Evaluation of High-Resolution Satellite Products for Streamflow and Water Quality Assessment in a Southeastern US Watershed." *Journal of Hydrology: Regional Studies* 27:100660. <https://doi.org/10.1016/j.ejrh.2019.100660>.
- Ashouri, H., K.-L. Hsu, S. Sorooshian, D. K. Braithwaite, K. R. Knapp, L. Dewayne Cecil, B. R. Nelson, and O. P. Prat. 2015. "Persiann-CDR: Daily Precipitation Climate Data Record from Multisatellite Observations for Hydrological and Climate Studies." *Bulletin of the American Meteorological Society* 96 (1): 69–83. <https://doi.org/10.1175/bams-d-13-00068.1>.
- Bartsotas, N. S., E. N. Anagnostou, E. I. Nikolopoulos, and G. Kallos. 2018. "Investigating Satellite Precipitation Uncertainty over Complex Terrain." *Journal of Geophysical Research Atmospheres* 123 (10): 5346–5359.
- Beck, H. E., E. F. Wood, M. Pan, C. K. Fisher, D. G. Miralles, A. I. J. M. van Dijk, T. R. McVicar, and R. F. Adler. 2019. "MSWEP V2 Global 3-Hourly 0.1° Precipitation: Methodology and Quantitative Assessment." *Bulletin of the American Meteorological Society* 100 (3): 473–500. <https://doi.org/10.1175/bams-d-17-0138.1>.

- Bezak, N., P. Borrelli, M. Mikoš, M. Jemec Auflič, and P. Panagos. 2024. "Towards Multi-Model Soil Erosion Modelling: An Evaluation of the Erosion Potential Method (EPM) for Global Soil Erosion Assessments." *Catena* 234:107596. <https://doi.org/10.1016/j.catena.2023.107596>.
- Bezak, N., P. Borrelli, and P. Panagos. 2022. "Exploring the Possible Role of Satellite-Based Rainfall Data in Estimating Inter- and Intra-Annual Global Rainfall Erosivity." *Hydrology and Earth System Sciences* 26 (7): 1907–1924. <https://doi.org/10.5194/hess-26-1907-2022>.
- Borrelli, P., P. Panagos, C. Alewell, C. Ballabio, H. de Oliveira Fagundes, N. Haregeweyn, E. Lugato, M. Maerker, J. Poesen, and M. Vanmaercke. 2023. "Policy Implications of Multiple Concurrent Soil Erosion Processes in European Farmland." *Nature Sustainability* 6 (1): 103–112.
- Chen, F., and Y. Gao. 2018. "Evaluation of Precipitation Trends from High-Resolution Satellite Precipitation Products Over Mainland China." *Climate Dynamics* 51:3311–3331. <https://doi.org/10.1007/s00382-018-4080-z>.
- Chen, F., X. Kong, X. Li, Y. Wang, and C. Pang. 2022. "Reliability of Satellite-Derived Precipitation Data in Driving Hydrological Simulations: A Case Study of the Upper Huaihe River Basin, China." *Journal of Hydrology* 612:128076. <https://doi.org/10.1016/j.jhydrol.2022.128076>.
- Chen, F., and X. Li. 2016. "Evaluation of IMERG and TRMM 3B43 Monthly Precipitation Products Over Mainland China." *Remote Sensing* 8 (6): 472.
- Chen, F. R., X. Li, and Y. G. Wang. 2025. "A Knowledge-Augmented Deep Fusion Method for Estimating Near-Surface Air Temperature." *Remote Sensing of Environment* 326:114819. <https://doi.org/10.1016/j.rse.2025.114819>.
- Chen, F., Y. Wang, and X. Li. 2024. "A Data-and Knowledge-Driven Method for Fusing Satellite-Derived and Ground-Based Precipitation Observations." *IEEE Transactions on Geoscience and Remote Sensing* 62:5301013. <https://doi.org/10.1109/TGRS.2024.3385647>.
- Chen, Y., M. Xu, Z. Wang, P. Gao, and C. Lai. 2021. "Applicability of Two Satellite-Based Precipitation Products for Assessing Rainfall Erosivity in China." *Science of the Total Environment* 757. <https://doi.org/10.1016/j.scitotenv.2020.143975>.
- Chi, Z., F. Chen, Y. Wang, C. Zhang, and G. Peng. 2023. "How Well Do 13 Satellite-Derived Precipitation Products Capture the Temporal and Spatial Variations of Precipitation Over Chinese Mainland?" *International Journal of Remote Sensing* 44 (22): 6981–7016. <https://doi.org/10.1080/01431161.2023.2277165>.
- Das, S., M. K. Jain, V. Gupta, R. P. McGehee, S. Yin, C. R. de Mello, and P. Panagos. 2024. "GloRESatE: A Dataset for Global Rainfall Erosivity Derived from Multi-Source Data." *Scientific Data* 11 (1). <https://doi.org/10.1038/s41597-024-03756-5>.
- Duan, Z., J. Liu, Y. Tuo, G. Chiogna, and M. Disse. 2016. "Evaluation of Eight High Spatial Resolution Gridded Precipitation Products in Adige Basin (Italy) at Multiple Temporal and Spatial Scales." *Science of the Total Environment* 573:1536–1553. <https://doi.org/10.1016/j.scitotenv.2016.08.213>.
- Funk, C., P. Peterson, M. Landsfeld, D. Pedreros, J. Verdin, S. Shukla, G. Husak, et al. 2015. "The Climate Hazards Infrared Precipitation with Stations—A New Environmental Record for Monitoring Extremes." *Science Data* 2:150066. <https://doi.org/10.1038/sdata.2015.66>.
- Gan, F., Y. Gao, L. Xiao, L. Qin, Y. Huang, and H. Zhang. 2020. "An Applicability Evaluation of Version 05 IMERG Precipitation Products Over a Coastal Basin Located in the Tropics with Hilly and Karst Combined Landform, China." *International Journal of Remote Sensing* 41 (12): 4570–4589.
- Gebremicael, T. G., Y. A. Mohamed, P. van der Zaag, A. Gebremedhin, G. Gebremeskel, E. Yazew, and M. Kifle. 2019. "Evaluation of Multiple Satellite Rainfall Products Over the Rugged Topography of the Tekeze-Atbara Basin in Ethiopia." *International Journal of Remote Sensing* 40 (11): 4326–4345.
- Golian, S., S. Moazami, P.-E. Kirstetter, and Y. Hong. 2015. "Evaluating the Performance of Merged Multi-Satellite Precipitation Products Over a Complex Terrain." *Water Resources Management* 29 (13): 4885–4901. <https://doi.org/10.1007/s11269-015-1096-6>.
- Gupta, H. V., H. Kling, K. K. Yilmaz, and G. F. Martinez. 2009. "Decomposition of the Mean Squared Error and NSE Performance Criteria: Implications for Improving Hydrological Modelling." *Journal of Hydrology* 377 (1–2): 80–91.
- Hou, X., J. Shao, X. Chen, J. Li, and J. Lu. 2020. "Changes in the Soil Erosion Status in the Middle and Lower Reaches of the Yangtze River Basin from 2001 to 2014 and the Impacts of Erosion on the Water Quality of Lakes and Reservoirs." *International Journal of Remote Sensing* 41 (8): 3175–3196.

- Huffman, G. J., D. T. Bolvin, D. Braithwaite, K. Hsu, R. Joyce, C. Kidd, S. Sorooshian, J. Tan, and P. Xie. 2020. "NASA Global Precipitation Measurement (GPM) Integrated Multi-satellitE Retrievals for GPM (IMERG)." *Algorithm Theoretical Basis Document (ATBD) Version 06*.
- Huffman, G. J., D. T. Bolvin, D. Braithwaite, K. Hsu, R. Joyce, P. Xie, and S.-H. Yoo. 2015. "NASA Global Precipitation Measurement (GPM) Integrated Multi-Satellite Retrievals for GPM (IMERG)." *Algorithm Theoretical Basis Document (ATBD) Version 4* (26): 30.
- Huffman, G. J., D. T. Bolvin, E. J. Nelkin, D. B. Wolff, R. F. Adler, G. Gu, Y. Hong, K. P. Bowman, and E. F. Stocker. 2007. "The TRMM Multisatellite Precipitation Analysis (TMPA): Quasi-Global, Multiyear, Combined-Sensor Precipitation Estimates at Fine Scales." *Journal of Hydrometeorology* 8 (1): 38–55. <https://doi.org/10.1175/jhm560.1>.
- Jiang, Q., W. Li, Z. Fan, X. He, W. Sun, S. Chen, J. Wen, J. Gao, and J. Wang. 2021. "Evaluation of the ERA5 Reanalysis Precipitation Dataset Over Chinese Mainland." *Journal of Hydrology* 595:125660. <https://doi.org/10.1016/j.jhydrol.2020.125660>.
- Joyce, R. J., J. E. Janowiak, P. A. Arkin, and P. Xie. 2004. "CMORPH: A Method That Produces Global Precipitation Estimates from Passive Microwave and Infrared Data at High Spatial and Temporal Resolution." *Journal of Hydrometeorology* 5 (3): 487–503.
- Keikhosravi-Kiany, M. S., S. Abolfazl Masoodian, R. C. Balling, and M. Darand. 2021. "Evaluation of Tropical Rainfall Measuring Mission, Integrated Multi-Satellite Retrievals for GPM, Climate Hazards Centre infrared Precipitation with Station Data, and European Centre for medium-Range Weather Forecasts Reanalysis V5 Data in Estimating Precipitation and Capturing Meteorological Droughts Over Iran." *International Journal of Climatology* 42 (4): 2039–2064. <https://doi.org/10.1002/joc.7351>.
- Kiany, K., M. Sadegh, S. Abolfazl Masoodian, R. C. Balling Jr, and M. Montazeri. 2020. "Evaluation of the TRMM 3B42 Product for Extreme Precipitation Analysis Over Southwestern Iran." *Advances in Space Research* 66 (9): 2094–2112. <https://doi.org/10.1016/j.asr.2020.07.036>.
- Koch, J., M. Cüneyd Demirel, and S. Stisen. 2018. "The SPATial Efficiency Metric (SPAEF): Multiple-Component Evaluation of Spatial Patterns for Optimization of Hydrological Models." *Geoscientific Model Development* 11 (5): 1873–1886.
- Lei, H., H. Zhao, and T. Ao. 2022. "Ground Validation and Error Decomposition for Six State-of-the-Art Satellite Precipitation Products over Mainland China." *Atmospheric Research* 269:106017. <https://doi.org/10.1016/j.atmosres.2022.106017>.
- Li, X., Z. Li, and Y. Lin. 2020. "Suitability of TRMM Products with Different Temporal Resolution (3-Hourly, Daily, and Monthly) for Rainfall Erosivity Estimation." *Remote Sensing* 12 (23). <https://doi.org/10.3390/rs12233924>.
- Li, Y., H. Yan, L. Chen, M. Huang, W. Shou, L. Zhu, L. Zhao, and Y. Xing. 2024. "Performance and Uncertainties of Five Popular Satellite-Based Precipitation Products in Drought Monitoring for Different Climate Regions." *Journal of Hydrology* 628:130562. <https://doi.org/10.1016/j.jhydrol.2023.130562>.
- Lin, Q., T. Peng, Z. Wu, J. Guo, W. Chang, and Z. Xu. 2022. "Performance Evaluation, Error Decomposition and Tree-Based Machine Learning Error Correction of GPM IMERG and TRMM 3B42 Products in the Three Gorges Reservoir Area." *Atmospheric Research* 268:105988. <https://doi.org/10.1016/j.atmosres.2021.105988>.
- Lu, X., G. Tang, M. Wei, L. Yang, and Y. Zhang. 2018. "Evaluation of Multi-Satellite Precipitation Products in Xinjiang, China." *International Journal of Remote Sensing* 39 (21): 7437–7462.
- Miao, C., H. Ashouri, K.-L. Hsu, S. Sorooshian, and Q. Duan. 2015. "Evaluation of the PERSIANN-CDR Daily Rainfall Estimates in Capturing the Behavior of Extreme Precipitation Events Over China." *Journal of Hydrometeorology* 16 (3): 1387–1396.
- Nearing, M. A., S.-Q. Yin, P. Borrelli, and V. O. Polyakov. 2017. "Rainfall Erosivity: An Historical Review." *Catena* 157:357–362. <https://doi.org/10.1016/j.catena.2017.06.004>.
- Nguyen, P., M. Ombadi, S. Sorooshian, K. Hsu, A. AghaKouchak, D. Braithwaite, H. Ashouri, and A. Rose Thorstensen. 2018. "The PERSIANN Family of Global Satellite Precipitation Data: A Review and Evaluation of Products." *Hydrology and Earth System Sciences* 22 (11): 5801–5816.
- Pradhan, R. K., Y. Markonis, M. Rodrigo Vargas Godoy, A. Villalba-Pradas, K. M. Andreadis, E. I. Nikolopoulos, S. Michael Papalexiou, A. Rahim, F. J. Tapiador, and M. Hanel. 2022. "Review

- of GPM IMERG Performance: A Global Perspective." *Remote Sensing of Environment* 268:112754. <https://doi.org/10.1016/j.rse.2021.112754>.
- Ruan, F., F. Chen, Q. Liu, and Z. Song. 2025. "Fusion of Satellite and Gauge Precipitation Observations through Coupling Spatio-Temporal Properties with Tree-Based Machine Learning." *Journal of Hydrology* 663:134240. <https://doi.org/10.1016/j.jhydrol.2025.134240>.
- Song, Y., T. Du, B. Zeng, Q. Wu, and G. Wang. 2024. "Evaluation of Fengyun Geosynchronous Orbit and GPM Satellites Precipitation Products Over the Southeastern Tibetan Plateau." *International Journal of Remote Sensing* 45 (16): 5616–5639.
- Taghizadeh, E., F. Ahmadi-Givi, L. Brocca, and E. Sharifi. 2021. "Evaluation of Satellite/Reanalysis Precipitation Products Over Iran." *International Journal of Remote Sensing* 42 (9): 3474–3497.
- Tan, M. L., A. Latif Ibrahim, Z. Duan, A. P. Cracknell, and V. Chaplot. 2015. "Evaluation of Six High-Resolution Satellite and Ground-Based Precipitation Products Over Malaysia." *Remote Sensing* 7 (2): 1504–1528.
- Tashima, T., T. Kubota, T. Mega, T. Ushio, and R. Oki. 2020. "Precipitation Extremes Monitoring Using the Near-Real-Time GSMaP Product." *IEEE Journal of Selected Topics in Applied Earth Observations & Remote Sensing* 13:5640–5651. <https://doi.org/10.1109/jstars.2020.3014881>.
- Teng, H., Z. Ma, A. Chappell, Z. Shi, Z. Liang, and W. Yu. 2017. "Improving Rainfall Erosivity Estimates Using Merged TRMM and Gauge Data." *Remote Sensing* 9 (11). <https://doi.org/10.3390/rs9111134>.
- Wan, Y., D. Li, J. Sun, M. Wang, and H. Liu. 2025. "Evaluation of Six Latest Precipitation Datasets for Extreme Precipitation Estimates and Hydrological Application Across Various Climate Regions in China." *Atmospheric Research* 315:107932. <https://doi.org/10.1016/j.atmosres.2025.107932>.
- Wang, J., L. Shunlin, and S. Peijun. 2022. "Topography and Landforms." In *The Geography of Contemporary China*, edited by J. Wang, S. Liang, and P. Shi, 63–84. Cham: Springer International Publishing.
- Wang, L., Y. Li, Y. Gan, L. Zhao, W. Qin, and L. Ding. 2024. "Rainfall Erosivity Index for Monitoring Global Soil Erosion." *Catena* 234:107593. <https://doi.org/10.1016/j.catena.2023.107593>.
- Xie, P., R. Joyce, S. Wu, S.-H. Yoo, Y. Yarosh, F. Sun, and R. Lin. 2017. "Reprocessed, Bias-Corrected CMORPH Global High-Resolution Precipitation Estimates from 1998." *Journal of Hydrometeorology* 18 (6): 1617–1641.
- Xie, Y., S.-Q. Yin, B.-Y. Liu, M. A. Nearing, and Y. Zhao. 2016. "Models for Estimating Daily Rainfall Erosivity in China." *Journal of Hydrology* 535:547–558. <https://doi.org/10.1016/j.jhydrol.2016.02.020>.
- Xu, X., Y. Yan, Q. Dai, X. Yi, Z. Hu, and L. Cen. 2023. "Spatial and Temporal Dynamics of Rainfall Erosivity in the Karst Region of Southwest China: Interannual and Seasonal Changes." *Catena* 221:106763. <https://doi.org/10.1016/j.catena.2022.106763>.
- Xu, Y., Z. Jiang, Y. Dai, Z. Li, Y. Liu, and L. Gu. 2024. "Ancient Wisdom: A New Perspective on the Past and Future Chinese Precipitation Patterns Based on the Twenty-Four Solar Terms." *Journal of Hydrology* 641:131873. <https://doi.org/10.1016/j.jhydrol.2024.131873>.
- Xu, Z., B. Pan, M. Han, J. Zhu, and L. Tian. 2019. "Spatial–Temporal Distribution of Rainfall Erosivity, Erosivity Density and Correlation with El Niño–Southern Oscillation in the Huaihe River Basin, China." *Ecological Informatics* 52:14–25. <https://doi.org/10.1016/j.ecoinf.2019.04.004>.
- Yan, Y., Z. Hu, L. Wang, J. Jiang, Q. Dai, F. Gan, A. H. Almaliki, M. A. Hashim, E. E. Hussein, and S. S. M. Ghoneim. 2024. "Impact of Extreme Rainfall Events on Soil Erosion on Karst Slopes: A Study of Hydrodynamic Mechanisms." *Journal of Hydrology* 638:131532. <https://doi.org/10.1016/j.jhydrol.2024.131532>.
- Yang, L., Z. Shi, R. Liu, and M. Xing. 2024. "Evaluating the Performance of Global Precipitation Products for Precipitation and Extreme Precipitation in Arid and Semiarid China." *International Journal of Applied Earth Observation and Geoinformation* 130:103888. <https://doi.org/10.1016/j.jag.2024.103888>.
- Yu, C., D. Hu, M. Liu, S. Wang, and Y. Di. 2020. "Spatio-Temporal Accuracy Evaluation of Three High-Resolution Satellite Precipitation Products in China Area." *Atmospheric Research* 241:104952. <https://doi.org/10.1016/j.atmosres.2020.104952>.
- Yu, R., T. Zhou, A. Xiong, Y. Zhu, and J. Li. 2007. "Diurnal Variations of Summer Precipitation Over Continuous China." *Geophysical Research Letters* 34 (1). <https://doi.org/10.1029/2006GL028129>.

- Yu, Y., W. Wei, L. Chen, T. Feng, and S. Daryanto. 2019. "Quantifying the Effects of Precipitation, Vegetation, and Land Preparation Techniques on Runoff and Soil Erosion in a Loess Watershed of China." *Science of the Total Environment* 652:755–764. <https://doi.org/10.1016/j.scitotenv.2018.10.255>.
- Zhan, C., Y. Chen, K. Yang, X. Zhou, Y. Jiang, X. Ling, J. Tian, Y. Wang, X. Li, and H. Yang. 2023. "First Evaluation of GPM-Era Satellite Precipitation Products with New Observations on the Western Tibetan Plateau." *Atmospheric Research* 283:106559. <https://doi.org/10.1016/j.atmosres.2022.106559>.
- Zhang, L., X. Chen, R. Lai, and Z. Zhu. 2022. "Performance of Satellite-Based and Reanalysis Precipitation Products Under Multi-Temporal Scales and Extreme Weather in Mainland China." *Journal of Hydrology* 605:127389. <https://doi.org/10.1016/j.jhydrol.2021.127389>.
- Zhang, L., X. Li, Y. Cao, Z. Nan, W. Wang, Y. Ge, P. Wang, and W. Yu. 2020. "Evaluation and Integration of the Top-Down and Bottom-Up Satellite Precipitation Products Over Mainland China." *Journal of Hydrology* 581:124456. <https://doi.org/10.1016/j.jhydrol.2019.124456>.
- Zhang, Y., Y. Chao, R. Fan, F. Ren, B. Qi, K. Ji, and B. Xu. 2021. "Spatial-Temporal Trends of Rainfall Erosivity and Its Implication for Sustainable Agriculture in the Wei River Basin of China." *Agricultural Water Management* 245:106557. <https://doi.org/10.1016/j.agwat.2020.106557>.
- Zhang, Y., C. Wu, J.-F. Pat, Y. J. Li, J. Li, B. X. Hu, and P. Feng. 2023. "Evaluating Drought Monitoring Utility of the Top-Down and Bottom-Up Satellite Precipitation Products Over Mainland China from a Three-Dimensional Perspective." *Journal of Hydrology* 625:130153. <https://doi.org/10.1016/j.jhydrol.2023.130153>.
- Zhang, Y., C. Wu, P. J. F. Yeh, J. Li, B. X. Hu, P. Feng, and C. Jun. 2022. "Evaluation and Comparison of Precipitation Estimates and Hydrologic Utility of CHIRPS, TRMM 3B42 V7 and PERSIANN-CDR Products in Various Climate Regimes." *Atmospheric Research* 265:105881. <https://doi.org/10.1016/j.atmosres.2021.105881>.
- Zhang, Y., C. Wu, P. J. F. Yeh, J. Li, B. X. Hu, P. Feng, and Y. Lei. 2022. "Evaluation of Multi-Satellite Precipitation Products in Estimating Precipitation Extremes Over Mainland China at Annual, Seasonal and Monthly Scales." *Atmospheric Research* 279:106387. <https://doi.org/10.1016/j.atmosres.2022.106387>.